Inorg. Chem. **2006**, *45*, 10347–10354

Stoichiometric and Catalytic Secondary O-Atom Transfer by Fe(III)–NO_2 Complexes Derived from a Planar Tetradentate Non-heme Ligand: Reminiscence of Heme Chemistry

Raman K. Afshar,[†] Aura A. Eroy-Reveles,[†] Marilyn M. Olmstead,[‡] and Pradip K. Mascharak*,[†]

Department of Chemistry and Biochemistry, University of California, Santa Cruz, California 95064, and Department of Chemistry, University of California, Davis, California 95616

Received July 27, 2006

An Fe(III) nitro complex [(bpb)Fe(NO_2)(py)] (**2**) of the tetradentate ligand 1,2-bis(pyridine-2-carboxamido)benzene (H_2bpb, H is the dissociable amide proton) has been synthesized via addition of $NaNO_2$ to [(bpb)Fe(py)$_2$](ClO_4) (**1**) in MeCN or DMF. This structurally characterized Fe(III) nitro complex exhibits its ν_{NO2} at 1384 cm^{-1}. The reaction of **1** with 2 equiv of Et_4NX (X = Cl^-, Br^-) affords the high-spin complexes (Et_4N)[(bpb)Fe(Cl_2)] (**3**) and (Et_4N)-[(bpb)Fe(Br_2)] (**4**), respectively. The structure of **4** has been determined. The addition of an equimolar amount of Et_4NCl, Et_4NBr, or Et_4NCN to a solution of **2** affords the mixed-ligand complexes (Et_4N)[(bpb)Fe(NO_2)(Cl)] (**5**), (Et_4N)[(bpb)Fe(NO_2)(Br)] (**6**), and (Et_4N)[(bpb)Fe(NO_2)(CN)] (**7**), respectively. These complexes are all low spin with isotropic *g* values of 2.15. Under anaerobic conditions, the reactions of **5**–**7** with Ph_3P in MeCN afford the five-coordinate {Fe–NO}^{7} nitrosyl [(bpb)Fe(NO)] (and Ph_3PO) via secondary oxygen-atom (O-atom) transfer. The O-atom transfer to Ph_3P by **5**–**7** becomes catalytic in the presence of dioxygen with transfer rates in the range of 1.70–13.59 × 10^{-3} min^{-1}. The O-atom transfer rates and turnover numbers (**5** > **6** > **7**) are reflective of the strength of the axial σ donors (Cl^- > Br^- > CN^-). The catalytic efficiencies of complexes **5**–**7** are limited due to formation of the thermodynamic end products [(bpb)Fe($X)_2]^-$ (where X = Cl^- for **5**, Br^- for **6**, and CN^- for **7**).

Introduction

The development of metal catalysts that activate dioxygen and promote oxygen atom (O-atom) transfer has received increasing attention because of its biological significance and potential industrial applications.[1−4] In general, O-atom transfer reactions can be classified into two categories, namely, primary and secondary O-atom transfer. Primary O-atom transfer, which proceeds via metal-oxo intermediates (M^{n+}=O, where *n* = 4 or 5 and M = Mn, Fe, Ru, or Re), have been utilized to oxidize a variety of substrates, such as carbon monoxide, phosphines, and olefins.[5−8] In secondary O-atom transfer reactions, the oxygen atom transferred to the substrate is derived from a coordinated ligand.[1,4] An important set of such O-atom transfer reactions employs a coordinated nitro (NO_2) group. To date, various Fe(III)−NO_2 and Co(III)−NO_2 complexes, mostly derived from porphyrin and porphyrin-like ligands (heme-type catalysts), have been used to oxidize a variety of substrates that include

* To whom correspondence should be addressed. E-mail: mascharak@chemistry.ucsc.edu.
† Department of Chemistry and Biochemistry, University of California, Santa Cruz.
‡ Department of Chemistry, University of California, Davis.

(1) (a) *Metal-Oxo and Metal-Peroxo Species in Catalytic Oxidations*; Meunier, B., Ed.; Structure and Bonding, Vol. 97; Springer: Berlin, 2000. (b) *Biomimetic Oxidations Catalyzed by Transition Metal Complexes*; Meunier, B., Ed.; Imperial College Press: London, 2000.
(2) (a) *Active Oxygen in Chemistry*, Foote, C. S., Valentine, J. S., Greenberg, A., Liebman, J. F., Eds.; Search Series, Vol. 2; Chapman & Hall: London, 1995. (b) *The Activation of Dioxygen and Homogeneous Catalytic Oxidation*; Barton, D. H. R., Martell, A. E., Sawyer, D. T., Eds.; Plenum: New York, 1993.
(3) Holm, R.H. *Chem. Rev.* **1987**, *87*, 1401−1449.
(4) (a) Sheldon, R. A.; Kochi, J. K. *Metal-Catalyzed Oxidation of Organic Compounds*; Academic Press: New York, 1981. (b) Spiro, T. G. *Metal Ion Activation of Dioxygen*; Wiley: New York, 1980.
(5) (a) Chin, D.-H.; La Mar, G. N.; Balch, A. L. *J. Am. Chem. Soc.* **1980**, *102*, 5945−5947. (b) Richman, R. M.; Peterson, M. W. *J. Am. Chem. Soc.* **1982**, *104*, 5795−5796.
(6) Miller, C. G.; Gordon-Wylie, S. W.; Horwitz, C. P.; Strazisar, S. A.; Periano, D. K.; Clark, G. R.; Weintraub, S. T.; Collins, T. J. *J. Am. Chem. Soc.* **1998**, *120*, 11540−11541.
(7) Chen, M. J.; Fremgen, D. E.; Rathke, J. W. *J. Porphyrins Phthalocyanines* **1998**, *2*, 473−482.
(8) Bhattacharya, S.; Chakraborty, I.; Dirghangi, B. K.; Chakravorty, A. *Inorg. Chem.* **2001**, *40*, 286−293.

10.1021/ic0614115 CCC: $33.50
Published on Web 11/08/2006

nitric oxide, nitrite, carbon monoxide, dioxygen, dimethyl sulfide, alkenes, alcohols, phosphines, and styrene via a nitro−nitrosyl redox couple.[9−17] The Fe(III)−NO_2 complexes have drawn special attention as biomimetic models of cytochrome P450 and nitrite reductase.[12,13] In contrast, the number of non-heme Fe(III)−NO_2 catalysts that undergo stoichiometric, as well as catalytic, O-atom transfer remains quite limited.[17]

Heme-type catalysts that promote secondary O-atom transfer reactions mostly consist of a "ferric heme" center (Fe(III) ligated to deprotonated H_2TPP, H_2TTP, H_2OEP, or H_2TpivPP)[18] with an axial NO_2^- group trans to a basic solvent ligand (such as pyridine or imidazole). The reaction of such six-coordinate Fe(III)−NO_2 complexes with an oxophillic substrate results in the formation of a five-coordinate {Fe−NO}^{7} intermediate,[19] and the solvent ligand dissociates from the metal center. Exposure to dioxygen and concomitant coordination of the solvent ligand regenerates the six-coordinate Fe(III)−NO_2 complex. For instance, Richter-Addo and co-workers have reported catalytic secondary O-atom transfer to Ph_3P by the nitro complex of the Fe(III) picket-fence porphyrin [(TpivPP)Fe(NO_2)(py)] in the presence of dioxygen.[15] In this reaction, the five-coordinate {Fe−NO}^{7} nitrosyl intermediate [(TpivPP)Fe(NO)] activates dioxygen in the presence of pyridine to re-form the six-coordinate [(TpivPP)Fe(NO_2)(py)] complex.

There are exceptions to the aforementioned secondary O-atom transfer in heme chemistry. For example, Goodwin and co-workers have reported that a bis(nitro) complex of Fe(III) picket-fence porphyrin [(TpivPP)Fe(NO_2)$_2$]$^-$ reacts with strong oxo-acceptors such as Ph_3P, NO, and thiophenols to form an six-coordinate {Fe−NO}^{7} intermediate [(TpiPP)Fe(NO)(NO_2)]$^-$.[14a] This six-coordinate {Fe−NO}^{7} intermediate will further react with dioxygen to re-form the [(TpivPP)Fe(NO_2)$_2$]$^-$ complex. Scheidt and co-workers, on the other hand, have shown that the reaction of BF_3·OEt_2 with the bis(nitro) complex of Fe(III) picket-fence porphyrin [K(18C6)(OH_2)][Fe(TpivPP)(NO_2)$_2$] leads to the formation of a five-coordinate intermediate [(TpivPP)Fe(NO_2)].[12c] This unstable species disproportionates to form [(TpivPP)Fe(NO_3)] and a five-coordinate {Fe−NO}^{7} nitrosyl [(TpivPP)Fe(NO)]. The five-coordinate {Fe−NO}^{7} nitrosyl further reacts with dioxygen to afford the five-coordinate intermediate [(TpivPP)Fe(NO_2)], which has also been structurally characterized.[12b] The O-atom transfer reaction continues until all of the {Fe−NO}^{7} nitrosyl [(TpivPP)Fe(NO)] has been transformed into [(TpivPP)Fe(NO_3)]. In this instance, dioxygen activation by the {Fe−NO}^{7} intermediate [(TpivPP)Fe(NO)] takes place in the absence of a sixth ligand.

The most efficient non-heme-type secondary O-atom transfer catalyst has been reported by Tovrog and co-workers.[10] This group has synthesized a Co(III)−NO_2 complex of the Schiff base salophen, namely, [(salophen)Co(NO_2)(py)], that undergoes catalytic O-atom transfer in the presence of Ph_3P and excess pyridine. This catalyst had a turnover number (TN) of 8.7 (at 60 °C) in 16 h, which is greater than TNs of any of the reported heme-type catalysts. The secondary O-atom transfer results in a five-coordinate {Co−NO}^{8} intermediate, [(salophen)Co(NO)], that is oxidized to the starting [(salophen)Co(NO_2)(py)] complex in the presence of dioxygen and pyridine.

We have recently reported an Fe(III)−NO_2 complex [($PaPy_3$)Fe(NO_2)](ClO_4) ($PaPy_3^-$ = deprotonated *N*,*N*-bis(2-pyridylmethyl)amine-*N*-ethyl-2-pyridine-2-carboxamide).[17] This non-heme-type catalyst transfers an O atom to Ph_3P in MeCN with a turnover number of 84 (at 65 °C) in 1 h. The exceptional efficiency of this non-heme catalyst is believed to arise from the strong σ donation of the trans-deprotonated carboxamido nitrogen.[17] The resulting six-coordinate {Fe−NO}^{7} nitrosyl [($PaPy_3$)Fe(NO)]$^+$ reacts with dioxygen to afford the [($PaPy_3$)Fe(NO_2)]$^+$ complex. In order to develop similar non-heme iron catalysts for secondary O-atom transfer and study the effect(s) of the σ-donor strength of the ligand trans to the nitro group, we have now synthesized and characterized three Fe(III)−NO_2 complexes of the type [(bpb)Fe(NO_2)(X)]$^-$ (bpb^{2-} = deprotonated 1,2-bis(pyridine-2-carboxamido) benzene; X = Cl^-, Br^-, CN^- for complexes **5**, **6**, and **7**, respectively) starting from [(bpb)Fe(NO_2)(py)] (**2**). The nature and efficiency of secondary O-atom transfer reactions to Ph_3P by these non-heme-type catalysts have been described in this account. The ligand H_2bpb is similar to porphyrin and its derivatives in that it is a conjugated tetradentate dianionic N4 donor. This similarity provides an opportunity to examine the rates and mechanisms of secondary O-atom transfer reactions by these complexes and compare them to the results reported with heme-type catalysts.

(9) Feltham, R. D.; Kreige, J. C. *J. Am. Chem. Soc.* **1979**, *101*, 5064−5065.

(10) (a) Tovrog, B. S.; Diamond, S. E.; Mares, F. *J. Am. Chem. Soc.* **1979**, *101*, 270−272. (b) Tovrog, B. S.; Mares, F.; Diamond, S. E. *J. Am. Chem. Soc.* **1980**, *102*, 6618−6619. (c) Tovrog, B. S.; Diamond, S. E.; Mares, F.; Szalkiewicz, A. *J. Am. Chem. Soc.* **1981**, *103*, 3522−3526. (d) Diamond, S. E.; Mares, F.; Szalkiewicz, A.; Muccigrosso, D. A.; Solar, J. P. *J. Am. Chem. Soc.* **1982**, *104*, 4266−4268.

(11) (a) Andrews, M. A.; Chang, T. C.-T.; Cheng, C.-W. F.; Emge, T. J.; Kelly, K. P.; Koetzle, T. F. *J. Am. Chem. Soc.* **1984**, *106*, 5913−5920. (b) Andrews, M. A.; Chang, T. C.-T.; Cheng, C.-W. F. *Organometallics.* **1985**, *4*, 268−274.

(12) (a) Finnegan, M. G.; Lappin, A. G.; Scheidt, R. W. *Inorg. Chem.* **1990**, *29*, 181−185. (b) Nasri, H.; Wang, Y.; Huynh, B. H.; Scheidt, R. W. *J. Am. Chem. Soc.* **1991,** *113*, 717−719. (c) Munro, O. Q.; Scheidt, R. W. *Inorg. Chem.* **1998**, *37*, 2308−2316.

(13) (a) Castro, C. E.; O'Shea, S. K. *J. Org. Chem.* **1995**, *60*, 1922−1923. (b) O'Shea, S. K. Wang, W.; Wade, R. S.; Castro, C. E. *J. Org. Chem.* **1996**, *61*, 6388−6395. (c) Castro, C. E. *J. Am. Chem. Soc.* **1996,** *118*, 3984−3985.

(14) (a) Frangione, M.; Port, J.; Murtuza, B.; Judd, A.; Galley, J.; DeVega, M.; Linna, K.; Caron. L.; Anderson, E. Goodwin, J. A. *Inorg. Chem.* **1997**, *36*, 1904−1911. (b) Goodwin, J.; Bailey, R.; Pennington, W.; Rasberry, R.; Green, T.; Shasho, S.; Yongsavanh, M.; Echevarria, V.; Tiedeken, J.; Brown, C.; Fromm, G.; Lyerly, S.; Watson, N.; Long, A.; De Nitto, N. *Inorg. Chem.* **2001**, *40*, 4217−4225.

(15) Cheng, L.; Powell, D. R.; Khan, M. A.; Richter-Addo, G. B. *Chem. Commun.* **2000**, 2301−2302.

(16) Adachi, H.; Suzuki, H.; Miyazaki, Y.; Limura, Y.; Hoshino, M. *Inorg. Chem.* **2002**, *41*, 2518−2524.

(17) Patra, A. K.; Afshar, R. K.; Rowland, J. M.; Olmstead, M. M.; Mascharak, P. K. *Angew. Chem.* **2003**, *115*, 4655−4659.

(18) Abbreviations: H_2TPP, tetraphenylporphyrin; H_2TTP, tetratolylporphyrin; H_2OEP, octaethylporphyrin; H_2TpivPP, *meso*-α,α,α,α-tetrakis(*o*-pivalamidophenyl)porphyrin.

(19) The {M−NO}^{n} notation used here is that of Feltham and Enemark where n is the sum of the d electrons of iron and the single π* electron of NO. See Enemark, J. H.; Feltham, R. D. *Coord. Chem. Rev.* **1974**, *13*, 339−406.

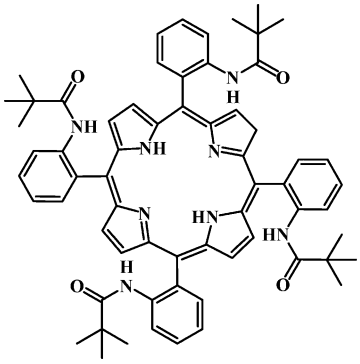

H_2TpivPP

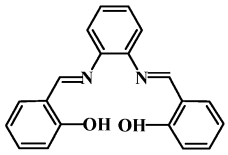

H_2Salophen

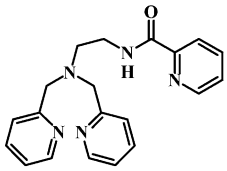

$PaPy_3H$

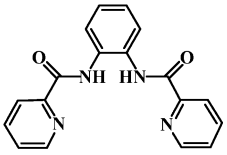

H_2bpb

Experimental Section

Sodium hydride (NaH), sodium nitrite ($NaNO_2$), tetraethylammonium bromide (Et_4NBr), tetraethylammonium chloride (Et_4NCl), tetraethylammonium cyanide (Et_4NCN), triphenylphosphine (Ph_3P), and triphenylphosphine oxide (Ph_3PO) were purchased from Aldrich Chemical Co. and used without further purification. The Fe(III) starting materials, $(Et_4N)[FeCl_4]$ and $[Fe(DMF)_6](ClO_4)_3$, were synthesized by following the published procedures.[20] H_2bpb (1,2-bis(pyridine-2-carboxamido)benzene), [(bpb)Fe(NO)], and Na-[(bpb)Fe$(CN)_2$] were synthesized by literature methods.[21,22] All of the solvents were purified, dried, or both by standard techniques and distilled prior to use.

Caution: Transition metal perchlorates should be handled with great caution and be prepared in small quantities because metal perchlorates are hazardous and may explode upon heating.

[(bpb)Fe(py)$_2$](ClO$_4$) (1). A slurry of 2.50 g (3.2 mmol) of [Fe-$(DMF)_6](ClO_4)_3$ in 20 mL of MeCN was added dropwise to a solution of 1.00 g (3.2 mmol) of H_2bpb and 1.00 g (12.6 mmol) of pyridine in 20 mL of MeCN. The red mixture was stirred for 1 h when the desired complex precipitated out from the reaction mixture as a dark red microcrystalline solid. The product was collected on a sintered glass funnel, washed with Et_2O and dried (yield: 1.4 g, 71%). Selected IR bands (KBr pellet, cm^{-1}): 3445 (m), 2369 (w), 1645 (s), 1626 (ν_{CO}, s), 1600 (ν_{CO}, s), 1446 (m), 1345 (s), 1296 (w), 1083 (s), 760 (m), 691 (w), 623 (w). Electronic absorption in MeCN, λ_{max}, nm (ϵ, M^{-1} cm^{-1}): 530 (1500), 325 (sh, 11 240).

[(bpb)Fe(NO$_2$)(py)]·0.5py (2·0.5py). Method A. A batch of 0.04 g (0.50 mmol) of $NaNO_2$ was added to a solution of 0.32 g (0.50 mmol) of $[(bpb)Fe(py)_2](ClO_4)$ in 30 mL of MeCN, and the mixture was stirred for 24 h. A dark red-brown microcrystalline compound separated from the solution during this time. The solid was filtered on a sintered glass frit, washed with Et_2O, and dried (yield: 0.19 g, 76%). Single crystals of **2** were obtained by slow diffusion of Et_2O into a 2:1 DMF/pyridine solution of **2** at − 20 °C. Anal. Calcd for $C_{25.5}H_{19.5}FeN_{6.5}O_4$ ([(bpb)Fe(NO_2)(py)]·0.5py): C, 57.05; H, 3.66; N, 16.96. Found: C, 57.01; H, 3.61; N, 16.93. Selected IR bands (KBr pellet, cm^{-1}): 3437 (w), 1627 (ν_{CO}, s), 1597 (ν_{CO}, s), 1470 (m), 1443 (m), 1384 (ν_{NO2}, s), 1353 (s), 1307 (m), 1138 (w), 813 (w), 757 (m), 690 (w). Electronic absorption in MeCN, λ_{max}, nm (ϵ, M^{-1} cm^{-1}): 830 (1400), 530 (sh 2300), 390 (sh 12 800), 310 (sh 19 200).

Method B. A solution of 0.01 g (0.12 mmol) of pyridine in 15 mL of MeCN was thoroughly degassed by freeze−pump−thaw cycles. Under positive N_2 pressure, a batch of 0.05 g (0.12 mmol) of [(bpb)Fe(NO)] was added, and the mixture was stirred for 15 min. Next, 5 mL of pure dioxygen was introduced (via gastight syringe) into the solution, and the mixture was stirred for 10 min when a dark red-brown solution resulted (λ_{max} = 830 nm). This solution afforded dark microcrystalline **2** upon further stirring (30 min) which was collected by filtration and washed with Et_2O and dried (yield: 0.04 g, 70%).

(Et$_4$N)[(bpb)Fe(Cl)$_2$] (3). Method A. A batch of 0.08 g (3.1 mmol) of NaH was added to slurry of 0.50 g (1.5 mmol) of H_2bpb in 50 mL of MeCN. The mixture became immediately homogeneous and turned yellow. The addition of a solution of 0.51 g (3.1 mmol) of $(Et_4N)[FeCl_4]$ in 30 mL of MeCN to this yellow solution afforded a green mixture. After the mixture was stirred for 2 h, the insoluble NaCl byproduct was removed using a sintered glass funnel. The homogeneous green solution of **3** was then concentrated to 20 mL under reduced pressure and stored at −20 °C. After 24 h, green microcrystals of **3** were collected on a sintered glass funnel, washed with Et_2O, and dried (yield: 0.72 g, 80%). Selected IR bands (KBr pellet, cm^{-1}): 3500 (w), 2980 (w) 2343 (w), 1621 (ν_{CO}, s), 1591 (ν_{CO}, s), 1565 (s), 1470 (m), 1447 (m), 1348 (s), 1290 (w), 1141 (w), 1042 (w), 942 (w), 750 (w). Electronic absorption in MeCN, λ_{max}, nm (ϵ, M^{-1} cm^{-1}): 680 (990), 350 (11 660).

Method B. A solution of 0.15 g (0.9 mmol) of Et_4NCl in 15 mL of MeCN was added dropwise to a solution of 0.30 g (0.5 mmol) of $[(bpb)Fe(py)_2](ClO_4)$ in 20 mL of MeCN. The color of the solution changed from dark red to green. It was stirred for an additional 1 h. Next, the volume of the solution was concentrated to 10 mL, and the dark green solution was stored at −20 °C. The green microcrystalline product (**3**) that separated from the solution was collected in a sintered glass funnel, washed with Et_2O, and dried (yield: 0.16 g, 60%).

(Et$_4$N)[(bpb)Fe(Br)$_2$] (4). A batch of 0.07 g (0.33 mmol) of Et_4-NBr was added to a solution of 0.10 g (0.16 mmol) of [(bpb)Fe-$(py)_2](ClO_4)$ in 8 mL of DMF. The mixture was stirred for 2 h when a green solution (λ_{max} = 750 nm) was obtained. The DMF was removed under vacuo, and the remaining residue was dissolved in 15 mL of MeCN. After the addition of 7 mL of Et_2O, the green solution was cooled at −20 °C for 48 h. The dark green crystals that separated during this time were collected on a sintered glass funnel, washed with Et_2O, and dried (yield: 0.07 g, 66%). Single crystals of **4** were grown via Et_2O diffusion into a dilute solution of **4** in MeCN. Anal. Calcd for $C_{26}H_{32}Br_2FeN_5O_2$ (Et_4N)[(bpb)-Fe$(Br)_2$]: C, 47.11; H, 5.22; N, 10.57. Found: C, 47.08; H, 5.26; N, 10.49. Selected IR bands (KBr pellet, cm^{-1}): 1613 (ν_{CO}, vs), 1590 (ν_{CO}, vs), 1567 (vs), 1472 (s), 1451 (s), 1350 (vs), 1290 (s), 1144 (m), 1042 (m), 767 (m), 693 (m), 644 (m). Electronic absorption in MeCN, λ_{max}, nm (ϵ, M^{-1} cm^{-1}): 750 (1510), 475 (sh, 3220), 355 (14 760).

(Et$_4$N)[(bpb)Fe(NO$_2$)(Cl)] (5). A batch of 0.01 g (0.04 mmol) of Et_4NCl was added to a vigorously stirring brown mixture of 0.02 g (0.04 mmol) of [(bpb)Fe(NO_2)(py)] in 10 mL of MeCN.

(20) (a) Hogkinson, J.; Jordan, R. B.; *J. Am. Chem. Soc.* **1973**, *95*, 763−768. (b) Sugimoto, H.; Sawyer, D. T. *J. Am. Chem. Soc.* **1985**, *107*, 5712−5716.

(21) Barnes, D. J.; Chapman, R. L.; Vagg, R. S.; Watton, E. C. *J. Chem. Eng. Data* **1978**, *23*, 349−350.

(22) Ray, M.; Mukherjee, R.; Richardson, J. F.; Buchanan, R. M. *J. Chem. Soc., Dalton Trans.* **1993**, 2451−2457.

Within 5 min, a homogeneous green solution with a λ_{max} of 720 nm was obtained. The volume of the green solution was then reduced to 5 mL, and 5 mL of Et_2O was added. The solution was stored at −20 °C for 24 h when the desired complex precipitated out as a green microcrystalline solid (yield: 0.02 g, 74%). Anal. Calcd for $C_{26}H_{32}ClFeN_6O_4$ (Et_4N)([(bpb)Fe(NO_2)(Cl)]: C, 53.47; H, 5.53; N, 14.39. Found: C, 53.41; H, 5.49; N, 14.42. Selected IR bands (KBr pellet, cm^{-1}): 3446 (w), 2980 (w) 2368 (w), 1620 (ν_{CO}, s), 1590 (ν_{CO}, s), 1565 (m), 1471 (m), 1447 (m), 1385 (s, ν_{NO2}), 1348 (s), 1313 (m), 1292 (w), 1143 (w), 1025(w), 943 (w), 764 (w).

(Et_4N)[(bpb)Fe(NO_2)(Br)] (6). This green complex was synthesized by following the procedure above except for the use of Et_4NBr instead of Et_4NCl (yield: 0.02 g, 65%). Anal. Calcd for $C_{26}H_{32}BrFeN_6O_4$ (Et_4N)([(bpb)Fe(NO_2)(Br)]: C, 49.68; H, 5.14; N, 13.38. Found: C, 49.65; H, 5.10; N, 13.42. Selected IR bands (KBr pellet, cm^{-1}): 3444 (w), 2981 (w), 1624 (ν_{CO}, s), 1592 (ν_{CO}, s), 1563 (m), 1470 (m), 1445 (m), 1384 (s, ν_{NO2}), 1348 (s), 1313 (m), 1292 (w), 1143 (w), 1025(w), 943 (w), 764 (w).

(Et_4N)[(bpb)Fe(NO_2)(CN)] (7). This green complex was synthesized by following the procedure above except for the use of Et_4NCN instead of Et_4NCl (yield: 0.02 g, 60%). Anal. Calcd for $C_{27}H_{32}FeN_7O_4$ (Et_4N)([(bpb)Fe(NO_2)(CN)]: C, 56.44; H, 5.62; N, 17.07. Found: C, 56.45; H, 5.61; N, 17.11. Selected IR bands (KBr pellet, cm^{-1}): 3448 (w), 2981 (w), 2250 (ν_{CN}, w), 1618 (ν_{CO}, s), 1592 (ν_{CO}, s), 1559 (m), 1471 (m), 1447 (m), 1384 (s, ν_{NO2}), 1348 (s), 1311 (m), 1292 (w), 1141 (w), 1023(w), 945 (w), 762 (w).

Conversion of the {Fe−NO}^{7} Nitrosyl [(bpb)Fe(NO)] to (Et_4N)[(bpb)Fe(NO_2)(Cl)] with Dioxygen. A solution of 0.02 g (0.12 mmol) of Et_4NCl and 0.01 g (0.12 mmol) of pyridine in 20 mL of MeCN was thoroughly degassed by freeze−pump−thaw cycles. Under positive N_2 pressure, a batch of 0.05 g (0.12 mmol) of [(bpb)Fe(NO)] was added, and the mixture was stirred for 15 min. Next, 5 mL of pure dioxygen was introduced (via gastight syringe) into the reaction mixture, and the mixture stirred for 10 min to yield a homogeneous green solution (λ_{max} = 720 nm). The volume of the green solution was reduced to 2 mL, and 5 mL of Et_2O was layered onto the green solution; it was then stored at −20 °C. Green microcrystals of (Et_4N)[(bpb)Fe(NO_2)(Cl)] (**5**) that precipitated from the solution were collected, washed with Et_2O, and dried (yield: 0.04 g, 49%). Selected IR bands (KBr pellet, cm^{-1}): 3446 (w), 2980 (w) 2368 (w), 1620 (ν_{CO}, s), 1590 (ν_{CO}, s), 1565 (s), 1471 (m), 1447 (m), 1385 (s, ν_{NO2}), 1348 (s), 1313 (m), 1292 (w), 1143 (w), 1025(w), 943 (w), 764 (w).

Stoichiometric O-Atom Transfer to Ph_3P by (Et_4N)[(bpb)-Fe(NO_2)(Cl)] and Formation of the {Fe−NO}^{7} Nitrosyl [(bpb)-Fe(NO)]. A batch of 0.04 g (0.07 mmol) of [(bpb)Fe(NO_2)(py)] was added to a solution of 0.01 g (0.07 mmol) of Et_4NCl in 20 mL of MeCN, and the brown mixture was stirred. After 20 min, the red-brown mixture became green (λ_{max} = 720 nm). Next, the green solution was thoroughly degassed via freeze−pump−thaw cycles. Under positive N_2 pressure, a batch of 0.02 g (0.07 mmol) of triphenylphosphine was added, and the solution was heated at 65 °C for 4 h. The color of the reaction mixture changed from green to brown. When the solution stood at room temperature for 2 h, dark brown microcrystals of [(bpb)Fe(NO)] separated from it. The product was collected, washed with Et_2O, and dried (yield: 0.02 g, 64%). Selected IR bands (KBr pellet, cm^{-1}): 3435 (w), 2980 (w), 1673 (m, ν_{NO}), 1634 (ν_{CO}, s), 1600 (ν_{CO}, s), 1575 (s), 1473 (m), 1453 (m), 1360, 1296 (w), 1140 (w), 1022(w), 962 (w), 760 (w). The other product of the reaction, namely, Ph_3PO, was collected by extraction of the dry residue of the reaction mixture with $CDCl_3$ (Figure S1).

Table 1. Summary of Crystal Data, Intensity Collection, and Structural Refinement Parameters for [(bpb)Fe(NO_2)(py)]·0.5py (**2**·0.5py) and (Et_4N)[(bpb)Fe($Br)_2$] (**4**)

formula	$C_{25.50}H_{19.50}FeN_{6.50}O_4$	$C_{26}H_{32}Br_2FeN_5O_2$
mol wt	536.83	662.24
cryst color, habit	black needle	black plate
T (K)	90(2)	90(2)
cryst syst	monoclinic	monoclinic
space group	$P2_1/c$	$P2_1$
a (Å)	15.7696(10)	8.7970(2)
b (Å)	10.0146(7)	10.7269(2)
c (Å)	15.6912(10)	15.0291(3)
α (deg)	90	90
β (deg)	112.451(2)	106.636(2)
γ (deg)	90	90
V (Å^3)	2290.2(3)	1358.85(5)
Z	4	2
d_{calcd} (g cm^{-3})	1.557	1.619
abs coeff (mm^{-1})	0.708	3.528
GOF[a] on F^2	1.050	0.849
R1[b] (%)	0.0699	0.0136
wR2[c] (%)	0.1661	0.0359

[a] GOF = $[\sum w(F_o^2 - F_c^2)^2]/(M - N)^{1/2}$ (M = no. of reflections, N = no. of parameters refined). [b] R1 = $\sum(||F_o| - |F_c||)/\sum|F_c|$ [c] wR2 = $[[\sum w(F_o^2 - F_c^2)^2]/\sum w(F_o)^2]^{1/2}$.

General O-Atom Transfer Reactions. To determine the rate of the O-atom transfer reaction by the [(bpb)Fe(NO_2)(X)]$^-$ catalysts, a 100:1 molar ratio of Ph_3P/Fe(III)−NO_2 complex was used. For example, a batch of 0.02 g (0.04 mmol) of [(bpb)Fe(NO_2)(py)] was added to a solution of 0.07 g (0.04 mmol) of Et_4NCl in 25 mL of MeCN. The mixture was stirred for 20 min when the typical dark green color (λ_{max} = 720 nm) of [(bpb)Fe(NO_2)(Cl)]$^-$ developed. Next, a batch of 1.05 g (4.0 mmol) of Ph_3P was added to the solution, and the reaction mixture was kept at 65 °C under 1 atm of dioxygen. Aliquots (100 μL) were taken out every 6 min and diluted to 10 mL with MeCN/H_2O (65:35). These samples were analyzed on a Spectra-Physics UV 2000 HPLC setup (Grace VYDAC reverse-phase C18 column, 5 μm particle size, 150 × 4.6 mm, 20 μL loop volume) using isocratic elution with MeCN/H_2O (65:35). Retention times for Ph_3PO and Ph_3P were 2.49 and 7.11 min, respectively (Figure S2). The areas under the peaks were determined with authentic samples of known concentration run under identical conditions. The rate was calculated from the slope of the plot of $-\ln [Ph_3P]_t/[Ph_3P]_o$ versus time (T). The turnover numbers (TNs) were calculated by dividing the number of moles of Ph_3PO by the number of moles of the catalyst.

Stability of (Et_4N)[(bpb)Fe(NO_2)(Cl)] (5). A batch of 0.04 g (0.07 mmol) of [(bpb)Fe(NO_2)(py)] was added to a solution of 0.01 g (0.07 mmol) of Et_4NCl in 20 mL of MeCN, and the brown reaction mixture was stirred. After 20 min, the brown mixture became a dark green homogeneous solution with a λ_{max} = 720 nm. Next, the dark green solution was heated for 30 min until it slowly became light green (λ_{max} = 680 nm). The solution was then stored at −20 °C for 24 h, resulting in the separation of green microcrystals of (Et_4N)[(bpb)Fe($Cl)_2$] (**3**) from the solution. The green product was washed with Et_2O and dried (yield: 0.02 g, 40%).

Other Physical Measurements. Electronic absorption spectra were recorded on a Perkin-Elmer Lambda 9 UV/Vis/NIR spectrophotometer. Infrared spectra were obtained with a Perkin-Elmer 1600 FTIR spectrometer. ^{31}P NMR spectra were monitored by a Varian Unity Plus spectrometer. Phosphoric acid was used as the internal standard in coaxial tube (δ for Ph_3P = −5 ppm and δ for Ph_3PO = 30 ppm in $CDCl_3$).

X-ray Data Collection and Structure Solution and Refinement. Reddish-brown blocks of **2**·0.5py were obtained by the diffusion of Et_2O into a concentrated solution of **2** in 2:1 DMF/

Table 2. Selected Bond Distances (Å) and Bond Angles (deg) for [(bpb)Fe(NO_2)(py)]·0.5py (**2**·0.5py) and (Et_4N)[(bpb)Fe(Br_2)] (**4**)

	[(bpb)Fe(NO_2)(py)]·0.5py (**2**·0.5py)		
Fe−N1	1.876(5)	C7−O1	1.241(7)
Fe−N2	1.883(5)	C13−02	1.251(7)
Fe−N3	2.000(5)	N5−O3	1.211(6)
Fe−N4	2.027(5)	N5−O4	1.245(6)
Fe−N5	1.945(5)	N1−C7	1.356(8)
Fe−N6	2.032(5)	N2−C13	1.348(8)
N1−Fe−N2	83.6(2)	N2−Fe−N6	93.3(2)
N1−Fe−N3	82.5(2)	N3−Fe−N4	111.9(2)
N1−Fe−N4	165.5(2)	N3−Fe−N5	87.6(2)
N1−Fe−N5	93.9(2)	N3−Fe−N6	88.96(19)
N1−Fe−N6	93.3(2)	N4−Fe−N5	88.5(2)
N2−Fe−N3	166.0(2)	N4−Fe−N6	85.59(19)
N2−Fe−N4	82.1(2)	N5−Fe−N6	171.6(2)
N2−Fe−N5	91.8(2)	O3−N5−O4	120.4(5)
	(Et_4N)[(bpb)Fe(Br_2)] (**4**)		
Fe−N1	2.0480(12)	C7−O1	1.2338(18)
Fe−N2	2.0458(12)	C13−02	1.2430(18)
Fe−N3	2.1695(12)	N1−C1	1.3997(19)
Fe−N4	2.1819(12)	N2−C2	1.4069(18)
Fe−Br1	2.5271(2)	N1−C7	1.3574(19)
Fe−Br2	2.5361(2)	N2−C13	1.3546(18)
N1−Fe−N2	77.88(5)	N2−Fe−Br2	101.02(3)
N1−Fe−N3	154.38(5)	N3−Fe−N4	128.61(5)
N1−Fe−N4	76.50(5)	N3−Fe−Br1	82.46(3)
N1−Fe−Br1	105.90(3)	N3−Fe−Br2	101.02(3)
N1−Fe−Br2	99.09(3)	N4−Fe−Br1	84.16(3)
N2−Fe−N3	76.96(5)	N4−Fe−Br2	82.83(3)
N2−Fe−N4	154.38(5)	Br1−Fe−Br2	148.181(10)
N2−Fe−Br1	103.21(4)		

pyridine at −20 °C, while green blocks of **4** were obtained via Et_2O diffusion into a dilute solution of **4** in MeCN at −20 °C. Diffraction data for both complexes were collected at 90 K on a Bruker SMART 100 system. Mo Kα (0.71073 Å) radiation was used, and the data were corrected for absorption effects. The structure was solved by direct methods (SHELXS-97). Machine parameters, crystal data, and data collection parameters for **2** and **4** are summarized in Table 1, while selected bond distances and angles are listed in Table 2. Complete crystallographic data for [(bpb)Fe(NO_2)(py)]·0.5py (**2**·0.5py) and (Et_4N)[(bpb)Fe(Br_2)] (**4**) have been submitted as Supporting Information.

Results and Discussion

Syntheses and Interconversions. The Fe(III) bis(pyridine) complex [(bpb)Fe(py_2)](ClO_4) (**1**) has been previously synthesized via the addition of [Fe($MeCN)_4$]($ClO_4)_2$ to an anaerobic solution of H_2bpb and pyridine in MeCN.[22] Exposure of this reaction mixture to dioxygen completes the synthesis and affords the desired Fe(III) complex **1**. We have now synthesized **1** using the Fe(III) starting salt [Fe($DMF)_6$]-($ClO_4)_3$. The use of the Fe(III) starting salt instead of the Fe(II) starting salt [Fe($MeCN)_{4]}$($ClO_4)_2$ affords **1** in high yield (71%) in a relatively convenient manner (no need for anaerobic manipulation). The addition of 1 equiv of $NaNO_2$ to a solution of **1** in MeCN or DMF affords the low-spin complex [(bpb)Fe(NO_2)(py)] (**2**) in a 76% yield. In addition, **2** can also be synthesized by introducing dioxygen to a solution containing the {Fe−NO}^{7} nitrosyl [(bpb)Fe(NO)][23] and 1 equiv of pyridine in MeCN.

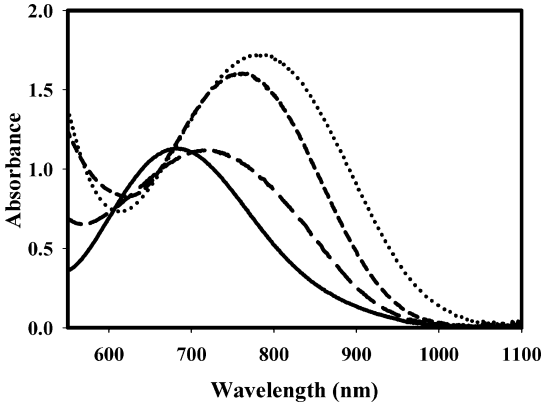

Figure 1. Changes in the electronic absorption spectra during the formation of the complexes (Et_4N)[(bpb)Fe(Cl_2)] (**3**, —), (Et_4N)[(bpb)Fe(NO_2)(Cl)] (**5**, - - -), (Et_4N)[(bpb)Fe(NO_2)(Br)] (**6**, - - -), and (Et_4N)[(bpb)Fe(NO_2)(CN)] (**7**, ···) in MeCN at 0.5 mM.

Addition of 2 equiv of Et_4NCl to a solution of **1** in MeCN affords the Fe(III) bis-chloro complex (Et_4N)[(bpb)Fe(Cl_2)] (**3**), whose structure was determined by Valentine and co-workers.[24] In the present work, we have synthesized **3** via the addition of (Et_4N)[$FeCl_4$] to a solution of H_2bpb and NaH in MeCN. The general route has been used to synthesize (Et_4N)[(bpb)Fe(Br_2)] (**4**) via the addition of 2 equiv of Et_4-NBr to a solution of **1** in DMF. The low solubility of Et_4-NBr in MeCN requires that the ligand displacement reaction be initially carried out in DMF. Complex **4** however can be recrystallized from MeCN in relatively good yield (66%).

The lability of the pyridine ligand in **2** allowed us to isolate the (Et_4N)[(bpb)Fe(NO_2)(X)] complexes (**5**−**7**) in a straightforward manner. The addition of an equimolar amount of the anionic ligands (in the form of Et_4NCl, Et_4NBr, or Et_4-NCN) to **2** in MeCN affords dark green homogeneous solutions (Figure 1) from which the target complexes can be isolated in analytically pure forms. Complexes **5**−**7** can also be synthesized from the {Fe−NO}^{7} nitrosyl [(bpb)Fe-(NO)]. For instance, the addition of 1 equiv of Et_4NCN to a solution of [(bpb)Fe(NO)] in MeCN containing 1 equiv of pyridine results in the formation of **7**, as evident by the development of the band with λ_{max} at 788 nm (Figure 1) and the ν_{CN} stretch at 2250 cm^{-1}. The anionic ligand X in **5**−**7** serves two functions, namely, (a) the solubility of the charged species greatly increases in MeCN and (b) the negative charge trans to the nitro group activates the process of O-atom transfer (vide infra). The substitution of the pyridine ligand by the anions (Cl^-, Br^-, and CN^-) is facile and occurs within 10 min. Complexes **5**−**7** are all low-spin complexes and exhibit isotropic EPR signals at $g = 2.15$. All three complexes decompose to the corresponding (Et_4N)[(bpb)-Fe(X_2)] species in solution upon heating. For instance, when **5** is heated in MeCN at 60 °C for 20 min, changes in the electronic absorption (λ_{max} shifts to 680 nm) indicates the formation of **3** in solution. These reactions are summarized in Scheme 1.

Structure of [(bpb)Fe(NO_2)(py)]·0.5py (2·0.5py). The structure of the Fe(III) nitro complex [(bpb)Fe(NO_2)(py)] (**2**)

(23) Patra, A. K.; Rose, M. J.; Olmstead, M. M.; Mascharak, P. K. *J. Am. Chem. Soc.* **2004**, *126*, 4780−4781.

(24) Yang, Y.; Diederich, F.; Valentine, J. S. *J. Am. Chem. Soc.* **1991**, *113*, 7195−7205.

Scheme 1. Summary of Reactions

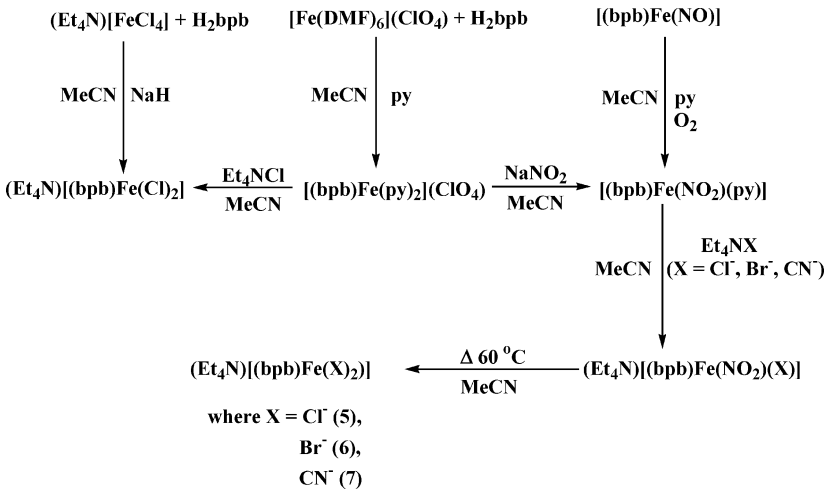

complex is shown in Figure 2, and selected bond distances and angles are listed in Table 2. The low-spin Fe(III) center is ligated to the four N atoms of the deprotonated bpb^{2-} ligand in the equatorial plane, while NO_2^- and py occupy the axial sites. Stronger coordination by the deprotonated carboxamido nitrogens to the Fe(III) center is evidenced by the shorter average $Fe-N_{amide}$ distance (1.8795(5) Å) compared to the average $Fe-N_{py}$ distance (2.020(5) Å) in the equatorial plane. The $Fe-N_{NO2}$ distance of **2** (1.945(5) Å) is much shorter than the $Fe-N_{NO2}$ distance of the $\{Fe-NO\}^6$ nitrosyl [(bpb)Fe(NO)(NO_2)] (2.0110(18) Å).[23] We attribute this to the strong trans effect of NO in [(bpb)Fe(NO)(NO_2)]. Comparison of the metric parameters of **2** with that of the heme analogue [(TpivPP)Fe(NO_2)(py)] reveals that the $Fe-N_{NO2}$ distance of **2** is shorter by ~0.015 Å than the $Fe-N_{NO2}$ distance of [(TpivPP)Fe(NO_2)(py)] (1.960(5) Å).[25] Also, the $Fe-N_{py}$ distance of **2** is slightly shorter than that of [(TpivPP)Fe(NO_2)(py)] (2.032(5) and 2.093 (5) Å, respectively). To the best of our knowledge, [(bpb)Fe(NO)(NO_2)] and **2** are the only examples of mononuclear low-spin Fe(III) complexes of bpb^{2-} (or related ligand systems) with mixed axial ligands systems.[23]

Structure of (Et_4N)[(bpb)Fe$(Br)_2$] (4). The structure of the bis-bromo Fe(III) complex (Et_4N)[(bpb)Fe$(Br)_2$] (**4**) is shown in Figure 3, and selected bond distances and angels are listed in Table 2. Much like **2**, the Fe(III) center is ligated to the four N atoms of the deprotonated bpb^{2-} ligand in the equatorial plane, while two Br^- ligands occupy the axial positions. Also, the average $Fe-N_{amide}$ distance (2.0469(12) Å) is shorter than the average $Fe-N_{py}$ distance (2.1757(12) Å). However, both the $Fe-N_{amide}$ and $Fe-N_{py}$ distances of **4** are longer than the corresponding distances of **2** because of the high-spin nature of the metal center. Interestingly, the Br−Fe−Br angle of **4** (148.181(10)°) is similar to the Cl−Fe−Cl angle of (Et_3HN)[(bpb)Fe$(Cl)_2$] (152.3(1)°).[24] Such bent Cl−Fe−Cl and Br−Fe−Br angles could arise from interactions of the anionic metal complexes with the Et_3HN^+ and Et_4N^+ cations in the crystal lattice.

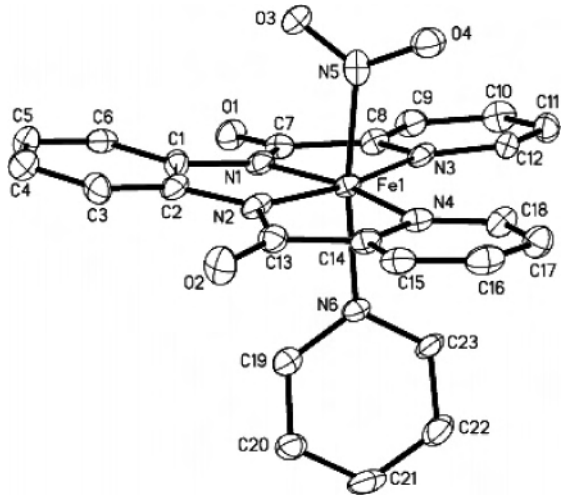

Figure 2. Thermal ellipsoid plot (probability level 50%) of [(bpb)Fe(py)(NO_2)] with the atom-labeling scheme. H atoms are omitted for the sake of clarity.

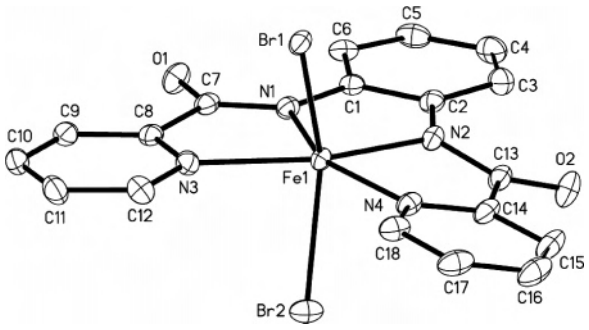

Figure 3. Thermal ellipsoid plot (probability level 50%) of (Et_4N)[(bpb)Fe$(Br)_2$] with the atom-labeling scheme. H atoms are omitted for the sake of clarity.

O-Atom Transfer Reactions with Ph_3P. Complexes **5**−**7** exhibit moderate O-atom transfer activity with Ph_3P. The rates of secondary O-atom transfer to Ph_3P and the turnover numbers (TN) are shown in Table 3. Although the rates and TNs are significantly higher than those reported for any Fe(III) nitro complex derived from porphyrin (or related) ligands,[13a,b,15] the O-atom transfer rates are still 10 times slower than that of $[(PaPy_3)Fe(NO_2)](ClO_4)$ reported by us

(25) Nasri, H.; Wang, Y.; Huynh, B. H.; Walker, F. A.; Scheidt, W. R. *Inorg. Chem.* **1991**, *30*, 1483−1489.

Table 3. Turnover Numbers and Rates of Secondary O-atom Transfer Reactions of [(bpb)Fe(NO_2)(py)] (**2**), (Et_4N)[(bpb)Fe(Cl_2)] (**3**), (Et_4N)[(bpb)Fe(Br_2)] (**4**) (Et_4N)[(bpb)Fe(NO_2)(Cl)] (**5**), (Et_4N)[(bpb)Fe(NO_2)(Br)] (**6**), (Et_4N)[(bpb)Fe(NO_2)(CN)] (**7**), and [($PaPy_3$)Fe(NO_2)](ClO_4) with Ph_3P in MeCN

complex	rate ($\times 10^{-3}$ min^{-1})	TN	ref
[(bpb)Fe(NO_2)(py)] (**2**), 65 °C	0	0	this work
(Et_4N)[(bpb)Fe(Cl_2)] (**3**), 65 °C	0	0	this work
(Et_4N)[(bpb)Fe(Br_2)] (**4**), 65 °C	0	0	this work
(Et_4N)[(bpb)Fe(NO_2)(Cl)] (**5**), 65 °C	1.70	10.0	this work
(Et_4N)[(bpb)Fe(NO_2)(Br)] (**6**), 65 °C	1.50	4.6	this work
(Et_4N)[(bpb)Fe(NO_2)(CN)] (**7**), 65 °C	1.10	2.2	this work
[($PaPy_3$)Fe(NO_2)](ClO_4), 45 °C	6.72	37.0	17
[($PaPy_3$)Fe(NO_2)](ClO_4), 65 °C	13.59	84.0	17

Scheme 2. Proposed Secondary O-Atom Mechanism Resulting in a Five-Coordinate {Fe−NO}^{7} Nitrosyl

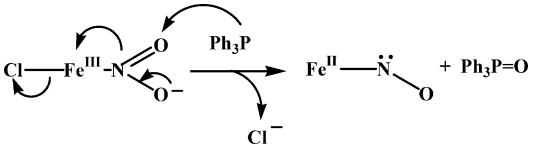

previously.[17] We attribute this to the inherent instability of the complexes **5**−**7**. As mentioned before, these mixed-ligand complexes decompose to the corresponding (Et_4N)[(bpb)-Fe(X_2)] species upon heating. Although [($PaPy_3$)Fe(NO_2)]-(ClO_4) also decomposes to the corresponding μ-oxo species upon heating, it is comparatively more robust, and hence the TN is much higher than those of the present complexes **5**−**7**.

Close scrutiny of Table 3 reveals an interesting trend when one compares the secondary O-atom transfer rates (and TNs) of **5**−**7**. As evident from the red shift of the λ_{max} of the LMCT band of these three complexes (Figure 1), the σ-donor strength of the trans ligands (Cl^-, Br^-, and CN^-) decreases in the order $Cl^- > Br^- > CN^-$. The rate of O-atom transfer is therefore directly proportional to the σ-donor strength of the ligand trans to the NO_2 unit. As the trans ligand becomes a weaker σ donor, the rate and TN of the O-atom transfer reaction drop significantly. Thus, **7** containing CN^- (strong π^* acceptor and a weak σ donor) exhibits the lowest rate and TN of all the O-atom transfer catalysts among all the nitro examples reported by us so far.

Stroichiometric secondary O-atom transfer reactions of **5**−**7** afford the five-coordinate {Fe−NO}^{7} intermediate [(bpb)Fe(NO)] (and Ph_3PO). For instance, when a solution of **5** and Ph_3P (1:1) in MeCN is heated at 60 °C under *anaerobic* conditions, the color of the reaction mixture changes from dark green to dark brown. When it stands at room temperature, a microcrystalline product separates from the solution that exhibits a ν_{CO} stretch at 1634 cm^{-1} and a ν_{NO} stretch at 1673 cm^{-1}. This IR spectrum is identical to that of an authentic sample of [(bpb)Fe(NO)].[23] The O-atom transfer reaction thus proceeds as shown in Scheme 2. Very similar behavior has been noted with [($PaPy_3$)Fe(NO_2)]-(ClO_4).[17]

The formation of the five-coordinate {Fe−NO}^{7} complex in secondary O-atom transfer reactions of **5**−**7** parallels the formation of a five-coordinate {FeNO}^{7} species noted in secondary O-atom transfer reactions by heme-type Fe(III)−NO_2 catalysts.[12c,13,14a,15] However, in many instances of secondary O-atom transfer reactions by such species, the axial ligands trans to the nitro group are solvent molecules that are easily displaced. Complexes **5**−**7** are the first examples in which the five-coordinate {Fe−NO}^{7} intermediate is formed via the displacement of anionic ligands (Cl^- for **5**, Br^- for **6**, and CN^- for **7**). The {Fe−NO}^{7} nitrosyl [(bpb)Fe(NO)] has no affinity for any exogenous ligands (such as Cl^-, Br^-, CN^-, and py). This is unlike the [(TPP)-Fe(NO)] complex which takes up free nitrite in solution to form the proposed [(TPP)Fe(NO)(ONO)]$^-$ species.[12a] The present work reveals that [(bpb)Fe(NO)] is a very stable species *in absence of dioxygen*. For example, a solution of

Scheme 3. Catalytic Secondary O-Atom Transfer to Ph_3P by **5**−**7**

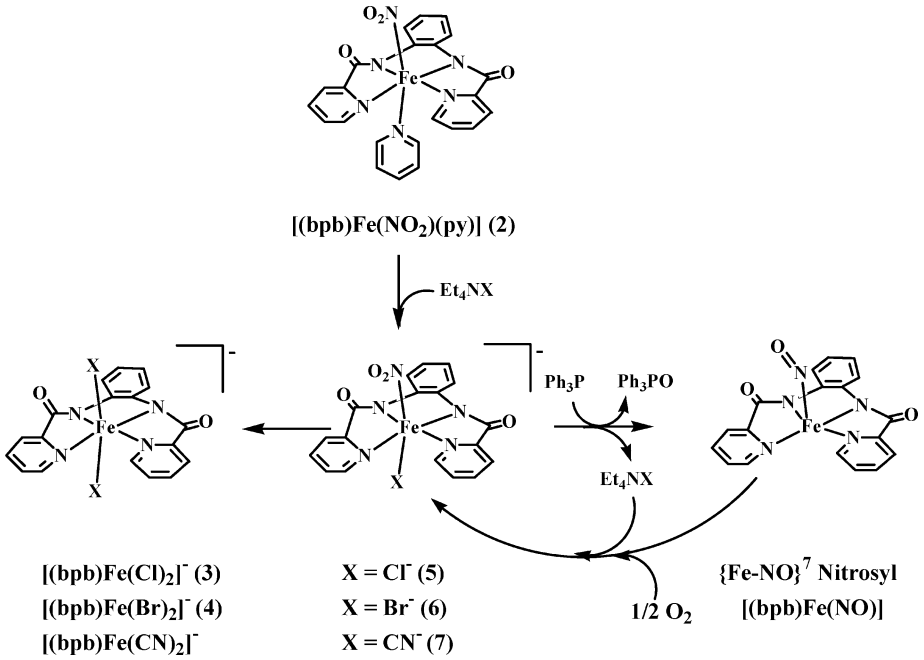

this $\{Fe-NO\}^7$ nitrosyl in MeCN remains unchanged in the presence of Et_4NCl even when it is heated at 60 °C for 24 h in the absence of dioxygen. No change is observed even if the reaction mixture contains excess pyridine and Ph_3P.

The exposure of a 1:1:1 mixture of [(bpb)Fe(NO)], pyridine, and Et_4NX (X = Cl^- for **5**, Br^- for **6**, and CN^- for **7**) in MeCN to dioxygen however rapidly regenerates the **5**−**7** complexes. Interestingly, the addition of just 1 equiv of Et_4NX (where X = Cl^-, Br^-, and CN^-) to a solution of [(bpb)Fe(NO)] in the presence of dioxygen affords the bis adducts, $(Et_4N)[(bpb)Fe(X)_2]$ (X = Cl^-, Br^-, or CN^-). At least one equivalent of pyridine is required for these solutions to exhibit the corresponding absorption bands for **5**−**7** in MeCN. It therefore appears that the presence of pyridine in the reaction mixture facilitates the formation of **2**, the species that eventually affords **5**−**7**. Regeneration of **5**−**7** in the reaction mixture under such conditions allowed us to run the secondary O-atom transfer reaction in a catalytic fashion. After the generation of **5**−**7** from **2** via addition of 1 equiv of Et_4NX in MeCN, secondary O-atom transfer reaction to Ph_3P was initiated by adding 100 equiv of Ph_3P (pseudo-first-order condition) and heating the reaction mixture at 65 °C under 1 atm of dioxygen (Scheme 3). The low TNs of the catalytic process (Table 3) indicate that **5**−**7**, much like other heme-type Fe(III)−NO_2 catalysts, are unstable and fail to continue catalytic secondary O-atom transfer via reversible $\{Fe-NO\}^7 \leftrightarrow$ Fe(III)−NO_2 transformation. The instability of the heme-type Fe(III)−NO_2 species has been known for quite some time.[12,13c] In a recent article, Ghosh and co-worker has attributed the instability to the "prodigiously electron-hungry nature of the Fe(III)−NO_2 species".[26] Results of their theoretical work suggest that such species relieve their electron affinities via O-atom transfer from the nitro group. It will be interesting to find out whether such comments are applicable to the non-heme Fe(III)−NO_2 species as well. Such studies are in progress at this time.

(26) Conradie, J.; Ghosh, A. *Inorg. Chem.* **2006**, *45*, 4902−4909.

Summary and Conclusions

The following are the summary and conclusions of the present work.

(1) A mixed-ligand Fe(III)−NO_2 complex derived from the tetradentate planar bpb^{2-} ligand, namely, $[(bpb)Fe(NO_2)(py)]$ (**2**), has been isolated and structurally characterized.

(2) The py ligand in **2** can be readily replaced by anionic ligands (X = Cl^-, Br^-, and CN^-) to afford complexes of the type $[(bpb)Fe(NO_2)(X)]^-$ (**5**−**7**) within 10 min at room temperature.

(3) The six-coordinate low-spin Fe(III) complexes **5**−**7** stoichiometrically transfer an O atom to Ph_3P in absence of dioxygen to afford the five-coordinate $\{Fe-NO\}^7$ nitrosyl [(bpb)Fe(NO)].

(4) In presence of dioxygen, complexes **5**−**7** catalytically transfer an O atom to Ph_3P via the reversible $\{Fe-NO\}^7 \leftrightarrow$ Fe(III)−NO_2 transformation. The rates of secondary O-atom transfer are directly proportional to the σ-donor strength of the ligand X trans to the nitro group. The rates of O-atom transfer are however slower than that of $[(PaPy_3)Fe(NO_2)](ClO_4)$, the only other non-heme-type catalyst reported previously.

(5) The moderate O-atom transfer capacity of **5**−**7** results from their instability in solution and conversion to $(Et_4N)[(bpb)Fe(X)_2]$ species (where X = Cl^-, Br^-, or CN^-).

Supporting Information Available: ^{31}P NMR spectrum of reaction mixture after O-atom transfer (Figure S1), HPLC trace of a typical reaction mixture showing formation of Ph_3PO (Figure S2), X-ray crystallographic data (in CIF format), and tables for the structure determination of $[(bpb)Fe(NO_2)(py)]\cdot 0.5py$ (**2**·0.5py) and $(Et_4N)[(bpb)Fe(Br)_2]$ (**4**). This material is available free of charge via the Internet at http://pubs.acs.org.

IC0614115